

## Derivatives of 4-Amino-6-hydroxy-2-mercaptopyrimidine as Novel, Potent, and Selective A<sub>3</sub> Adenosine Receptor Antagonists

Barbara Cosimelli,<sup>\*,†</sup> Giovanni Greco,<sup>†</sup> Marina Ehlardo,<sup>†</sup> Ettore Novellino,<sup>†</sup> Federico Da Settimo,<sup>§</sup> Sabrina Taliani,<sup>§</sup> Concettina La Motta,<sup>§</sup> Marusca Bellandi,<sup>§</sup> Tiziano Tuccinardi,<sup>§</sup> Adriano Martinelli,<sup>§</sup> Osele Ciampi,<sup>‡</sup> Maria Letizia Trincavelli,<sup>‡</sup> and Claudia Martini<sup>‡</sup>

*Dipartimento di Chimica Farmaceutica e Tossicologica, Università di Napoli "Federico II", Via D. Montesano, 49, 80131 Napoli, Italy, Dipartimento di Scienze Farmaceutiche, Università di Pisa, Via Bonanno 6, 56126 Pisa, Italy, and Dipartimento di Psichiatria, Neurobiologia, Farmacologia e Biotecnologie, Università di Pisa, Via Bonanno 6, 56126 Pisa, Italy*

Received September 17, 2007

A number of derivatives of 4-amino-6-hydroxy-2-mercaptopyrimidine (**5**) were synthesized and biologically evaluated as A<sub>3</sub> adenosine receptor (A<sub>3</sub> AR) antagonists. The new compounds were designed as open chain analogues of a triazolopyrimidinone derivative displaying submicromolar affinity for the A<sub>3</sub> AR, which had been previously identified using a 3D database search. Substituents R, R', and R'' attached to the parent compound **5** were chosen according to factorial design and stepwise lead optimization approaches, taking into account the essentially hydrophobic nature of the A<sub>3</sub> AR binding site. As a result, **5m** (R = *n*-C<sub>3</sub>H<sub>7</sub>, R' = 4-ClC<sub>6</sub>H<sub>4</sub>CH<sub>2</sub>, R'' = CH<sub>3</sub>) was identified among the pyrimidine derivatives as the ligand featuring the best combination of potency and selectivity for the target receptor. This compound binds to the A<sub>3</sub> AR with a K<sub>i</sub> of 3.5 nM and is devoid of appreciable affinity for the A<sub>1</sub>, A<sub>2A</sub>, and A<sub>2B</sub> ARs.

### Introduction

Adenosine is a ubiquitous purine nucleoside that plays a pivotal role in a large variety of physiological and pathophysiological processes, which are modulated by its interaction with specific receptors. Four different adenosine receptors (ARs) have been identified, A<sub>1</sub>, A<sub>2A</sub>, A<sub>2B</sub>, and A<sub>3</sub>, all of which belong to the superfamily of G-protein-coupled receptors.<sup>1–3</sup> ARs from different species show 82–92% amino acid sequence homology, the only exception being the A<sub>3</sub> AR, which exhibits 74% homology between rats and humans.<sup>4–6</sup>

AR-mediated signaling occurs through inhibition (A<sub>1</sub> and A<sub>3</sub>) or stimulation (A<sub>2A</sub> and A<sub>2B</sub>) of adenylate cyclase, resulting in a modification of the intracellular production of cAMP. Adenosine receptor coupling to other second messenger systems has also been described, such as stimulation of phospholipase C (A<sub>1</sub>, A<sub>2B</sub>, and A<sub>3</sub>) or activation and inhibition of potassium and calcium channels (A<sub>1</sub>).<sup>7</sup>

Each AR is considered an attractive target for pharmacological intervention in many pathological conditions, including renal failure, cardiac and cerebral ischemia, central nervous system disorders, neurodegenerative diseases, and inflammatory pathologies, such as asthma.<sup>8</sup> The development of potent and selective synthetic antagonists of ARs has been the subject of medicinal chemistry research for more than 3 decades.<sup>9</sup> In particular, over the past few years, the interest in blocking the A<sub>3</sub> subtype increased after the discovery of its involvement in cellular growth.<sup>10</sup>

The A<sub>3</sub> AR is widely distributed in mammals, but pronounced differences in expression levels exist between species. In humans, the highest density of this receptor has been found in lung and liver, with lower levels in aorta, brain, and testes.<sup>11</sup>

The A<sub>3</sub> AR is involved in a variety of important physiological processes, including modulation of cerebral and cardiac ischemic damage,<sup>11,12</sup> inflammation,<sup>13</sup> modulation of intraocular pressure,<sup>14</sup> regulation of normal and tumor cell growth,<sup>10,15,16</sup> and immunosuppression.<sup>2,17</sup> Accordingly, A<sub>3</sub> AR antagonists may be employed in the acute treatment of stroke and glaucoma and as antiasthmatic, antiallergenic, and cerebroprotective agents.<sup>17</sup> Furthermore, the significant overexpression of A<sub>3</sub> AR in several types of tumor cells and the pro-survival and antiapoptotic effects of A<sub>3</sub> AR stimulation have recently led Baraldi et al. to propose that antagonists for this receptor might sensitize tumor cells to chemotherapeutic drugs.<sup>15,18</sup>

In the past 5 years, considerable progress has been made toward the identification and development of potent and selective ligands for A<sub>3</sub> AR. The best known classes of A<sub>3</sub> AR antagonists (see Chart 1) are imidazopyrimidines **I**,<sup>19,20</sup> triazoloquinazolines **II**,<sup>21,22</sup> pyrazolotriazolopyrimidines **III**,<sup>15,23,24</sup> triazoloquinoxalines **IV** and **V**,<sup>25–27</sup> isoquinolines **VI**,<sup>28–30</sup> and pyridines **VII**.<sup>31–33</sup>

We have recently described the synthesis and the biological evaluation of a number of A<sub>1</sub> and A<sub>3</sub> AR antagonists designed using database search and lead optimization approaches (structures and binding data are reported in Table 1).<sup>34</sup> Our work proceeded through the following steps (Figure 1). Briefly, (i) the Cambridge Structural Database (CSD)<sup>35</sup> was searched using two substructures as queries extracted by known A<sub>1</sub> and A<sub>3</sub> AR antagonists; (ii) five potential leads (**A–E**) were selected to purchase, synthesize, or translate synthetically into less bulky or hydrophilic analogues; (iii) out of the five tested compounds, two displayed micromolar to nanomolar affinity for the A<sub>1</sub> AR (**B** and **C**), four showed nanomolar affinity for the A<sub>3</sub> R (**B–E**), while one turned out to be inactive (**A**); (iv) lead optimization efforts gave the best results in the series of 2-(benzimidazol-2-yl)quinoxalines (**C**) yielding compounds **C'** and **C''** as potent and selective antagonists at the A<sub>1</sub> and A<sub>3</sub> ARs, respectively.

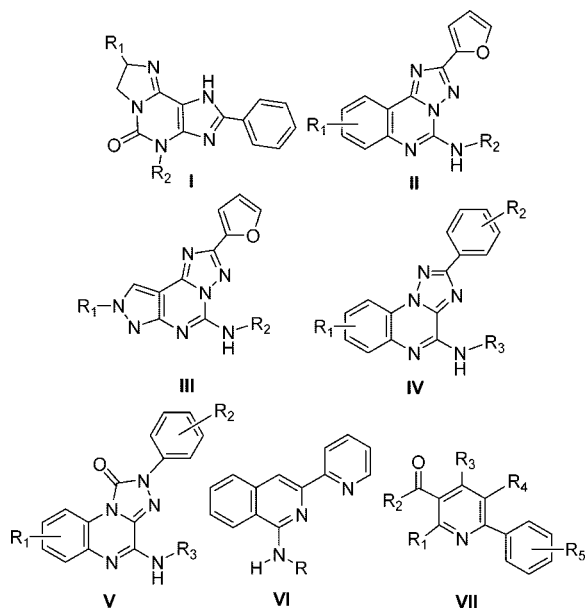
Although the triazolopyrimidinone **E** exhibited an interesting selectivity profile at the A<sub>3</sub> AR, simple modifications about the thiazolidine ring yielded compounds equipotent or

\* To whom correspondence should be addressed. Phone: 081678614. Fax: 081678630. E-mail: barbara.cosimelli@unina.it.

<sup>†</sup> Università di Napoli "Federico II".

<sup>§</sup> Dipartimento di Scienze Farmaceutiche, Università di Pisa.

<sup>‡</sup> Dipartimento di Psichiatria, Neurobiologia, Farmacologia e Biotecnologie, Università di Pisa.

Chart 1. Structures of Known A<sub>3</sub> AR Antagonists

**Table 1.** Affinities at Human A<sub>1</sub>, A<sub>2A</sub>, and A<sub>3</sub> ARs of Compounds Designed as A<sub>1</sub> AR and/or A<sub>3</sub> AR Antagonists by Means of 3D Database Searching<sup>34</sup>

compd	K <sub>i</sub> (nM) <sup>a</sup>		
	hA <sub>1</sub> <sup>b</sup>	hA <sub>2A</sub> <sup>c</sup>	hA <sub>3</sub> <sup>d</sup>
<b>A</b>	>10000	>10000	>1000
<b>B</b>	3336 ± 557	>10000	125 ± 20
<b>C</b> (R = H)	50 ± 15	561 ± 17	763 ± 13
<b>C'</b> (R = SC <sub>2</sub> H <sub>5</sub> )	0.5 ± 0.01	3440 ± 980	955 ± 215
<b>C''</b> (R = CH <sub>3</sub> )	8000 ± 567	833 ± 67	26 ± 9
<b>D</b>	>10000	>10000	130 ± 3
<b>E</b> <sup>e</sup>	>10000	>10000	440 ± 33
DPCPX <sup>f</sup>	0.5 ± 0.03	337 ± 28	>1000
NECA <sup>g</sup>	14 ± 4	16 ± 3	73 ± 5
CI-IB-MECA <sup>h</sup>	890 ± 61	401 ± 25	0.22 ± 0.02

<sup>a</sup> The K<sub>i</sub> values are the mean ± SEM of at least three determinations derived from an iterative curve-fitting procedure (Prism program, GraphPad, San Diego, CA). <sup>b</sup> Displacement of specific [<sup>3</sup>H]DPCPX binding in membranes obtained from CHO cells stably expressing hA<sub>1</sub> AR. <sup>c</sup> Displacement of specific [<sup>3</sup>H]NECA binding in membranes obtained from CHO cells stably expressing hA<sub>2A</sub> AR. <sup>d</sup> Displacement of specific [<sup>125</sup>I]AB-MECA binding in membranes obtained from CHO cells stably expressing hA<sub>3</sub> AR. <sup>e</sup> Assayed with a purity degree of 96%. <sup>f</sup> DPCPX: 1,3-dipropyl-8-cyclopentyl-xanthine. <sup>g</sup> NECA: 5'-N-ethylcarboxamidoadenosine. <sup>h</sup> CI-IB-MECA: 2-chloro-N<sup>6</sup>-(3-iodobenzyl)adenosine-5'-N-methylcarboxamide.

inactive in binding experiments. Because the triazolopyrimidinone scaffold was not synthetically versatile, we turned our attention to derivatives of 4-amino-6-hydroxy-2-mercaptopyrimidine (**5**) and 6-amino-2-mercaptopyrimidin-4(3H)-one (**6**) as open chain analogues of **E**, which were better suited to lead optimization (Figure 2). Taking into account that the binding site of A<sub>3</sub> AR antagonists is mostly lipophilic,

the R, R', and R'' substituents in the general formulas **5** and **6** were alkyl and phenylalkyl chains.

Preliminary binding assays of the first newly synthesized compounds revealed that derivatives of series **6** were totally devoid of any affinity toward ARs (data not shown) while derivatives of series **5** displayed interesting binding profiles at the A<sub>3</sub> AR. A few precursors of series **5** (**4d,e**) and **6** (**3d,e**) likewise turned out to be inactive (data not shown). Further research focused on series **5** through the design, synthesis, and testing of additional 4-amino-6-hydroxy-2-mercaptopyrimidines to identify those characterized by the highest affinity and selectivity as A<sub>3</sub> AR antagonists.

## Chemistry

The derivatives **5a–s** were obtained in three steps starting from the commercially available 4-amino-6-hydroxy-2-mercaptopyrimidine monohydrate (**1**) (Scheme 1). The first was the alkylation of the sulfur atom at the 2-position by reaction with iodomethane or the opportune bromo(phenyl)alkane in 1 M NaOH to give compounds **2a–e** (Table 1 of Supporting Information), which were collected by filtration and were sufficiently pure to be used in the next step without further purification. The second step, i.e., the alkylation of the 4-oxygen atom of compounds **2a–e** to prepare derivatives **4**, always gave a mixture of the isomeric products **3** and **4** because of the keto–enol equilibrium of the pyrimidinone scaffold. The experimental conditions were extensively studied with regard to solvent (anhydrous DMF, acetonitrile, ...), base quantities, temperature, and time of reaction. The best results in terms of **4** yields were obtained when the reaction was carried out in anhydrous DMF in the presence of an excess of K<sub>2</sub>CO<sub>3</sub> as base, which generally gave a 1:3 ratio of the isomers obtained varied depending on the stereoelectronic features of both reagents. Conversely, for example, the use of acetonitrile as solvent increased the formation of the **3** isomer. For only the case of derivatives with R' = CH<sub>3</sub>, the use of methyl iodide always gave an excess of the N-isomer **3** with respect to **4** (see Table 2 of Supporting Information for details). The **4** isomer was then easily isolated by flash chromatography and characterized (Tables 2 and 3 of Supporting Information). The final step was the conversion of the 4-amino group of **4** into the amide group of **5** by reaction with the opportune anhydride and concentrated H<sub>2</sub>SO<sub>4</sub> as catalyst (Table 4 of Supporting Information).

## Biology

The affinities of the new compounds **5a–s** toward human A<sub>1</sub>, A<sub>2A</sub>, and A<sub>3</sub> ARs were evaluated by competition experiments assessing their respective abilities to displace [<sup>3</sup>H]DPCPX, [<sup>3</sup>H]NECA, or [<sup>125</sup>I]AB-MECA binding from transfected Chinese hamster ovary (CHO) cells. Experiments were performed as described elsewhere.<sup>36</sup>

Compounds **5m**, **5o**, **5p**, and **5r**, which all showed high A<sub>3</sub> affinity, were also tested in functional assays at human A<sub>2B</sub> and A<sub>3</sub> ARs by measuring their effects on NECA-mediated cAMP modulation in transfected CHO cells.<sup>37</sup>

## Results and Discussion

Table 2 lists the binding affinities for the human A<sub>1</sub>, A<sub>2A</sub>, and A<sub>3</sub> ARs of the new derivatives of 4-amino-6-hydroxy-2-mercaptopyrimidine (**5a–s**). The first eight compounds (**5a–h**) were prepared according to a factorial design in which the size/lipophilicity of substituents R, R', and R'' was explored at two levels. For R and R' the low and high levels correspond to CH<sub>3</sub>

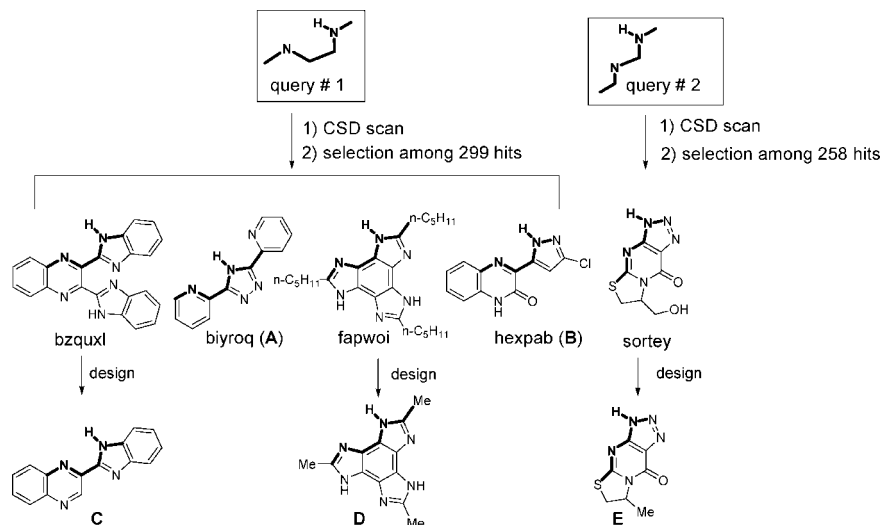


**Figure 1.** Strategy adopted to identify lead compounds as antagonists at the  $A_1$  and/or  $A_3$  ARs by a 3D search of the CSD.

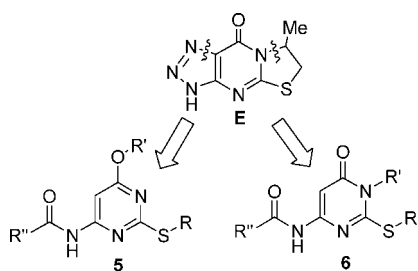
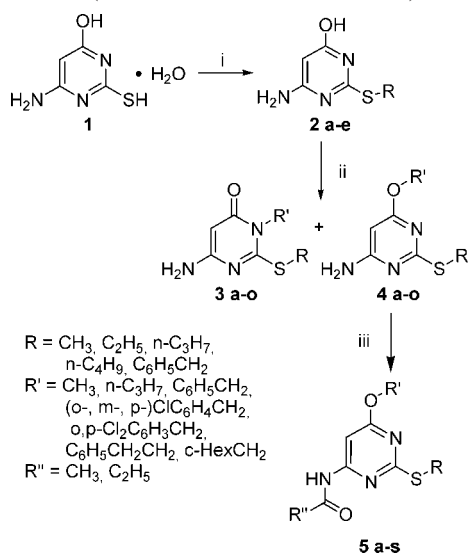


**Figure 2.** Design of open-chain analogues of triazolopyrimidinone **E** as potential  $A_3$  AR antagonists.

**Scheme 1.** Synthesis of 4-Amino-6-hydroxy-2-mercaptopyrimidine Derivatives **5a–s** (See Table 2 for the Substituents)<sup>a</sup>



<sup>a</sup> Reagents and conditions: (i) methyl iodide or (phenyl)alkyl bromide, 1 M NaOH; (ii) methyl iodide or (substituted phenyl)alkyl bromide, anhydrous DMF, excess  $\text{K}_2\text{CO}_3$ ; (iii) acetic or propionic anhydride, catalytic conc  $\text{H}_2\text{SO}_4$ .

and  $n\text{-C}_3\text{H}_7$ , respectively; for  $R''$  the low and high levels correspond to  $\text{CH}_3$  and  $\text{C}_2\text{H}_5$ , respectively. The best combination of substituents was found in **5g** ( $R = R' = n\text{-C}_3\text{H}_7$ ,  $R'' = \text{CH}_3$ ), which displayed a  $K_i$  value of 26 nM at the  $A_3$  AR, submicromolar affinity at the  $A_1$  AR, and no affinity at the  $A_{2A}$  AR.

The binding data of **5a–h** suggest that the effects of  $R$ ,  $R'$ , and  $R''$  on  $A_3$  AR affinity are fairly additive and that selectivity

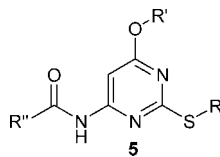
for  $A_3$  AR versus  $A_{2A}$  AR is conferred by a large  $R'$  and a small  $R''$  (compare **5g** vs **5h**). Moreover, a pairwise comparison of the couples **5c,d**, **5e,f**, and **5h,g** indicates that switching of  $R''$  from  $\text{CH}_3$  to  $\text{C}_2\text{H}_5$  slightly lowers affinity for  $A_3$  AR. Thus, further modifications of  $R''$  were not taken into consideration.

Taking **5g** as the reference structure, further modifications were made to increase potency and selectivity at the  $A_3$  AR. First, we inserted a bulky benzyl group on the S-2 atom, obtaining **5i**, which showed a significant decrease in affinity for the target receptor. Then, by keeping fixed  $R = n\text{-C}_3\text{H}_7$  and  $R'' = \text{CH}_3$ , we increased the weight of  $R'$  through substituted benzyl chains (compounds **5j–o**). This modification produced a general enhancement in  $A_3$  AR affinity, with **5o** ( $R' = 4\text{-CH}_3\text{OC}_6\text{H}_4\text{CH}_2$ ) being the most active compound ( $K_i = 1.8$  nM). Within this subset, **5m** ( $R' = 4\text{-ClC}_6\text{H}_4\text{CH}_2$ ) was the best-performing derivative compared with **5g**, showing a  $K_i$  of 3.5 nM at the  $A_3$  AR and no affinity for  $A_1$  and  $A_{2A}$  ARs. Additional modifications of  $R'$  led to the synthesis of **5p** and **5q**, featuring a  $\text{PhCH}_2\text{CH}_2$  and a  $c\text{-HexCH}_2$  chain, respectively. Although these two compounds showed excellent affinity (**5p** was the most active compound of the whole series with a  $K_i$  of 1.4 nM) and selectivity at the  $A_3$  AR, they were not significantly better than **5m**.

Finally, to find the optimum size/lipophilicity of  $R$ , we took **5m** as the reference structure and replaced the  $n\text{-C}_3\text{H}_7$  with a  $\text{C}_2\text{H}_5$  or a  $n\text{-C}_4\text{H}_9$  to obtain **5r** and **5s**, respectively. Both compounds exhibited nanomolar potency at the  $A_3$  AR ( $K_i$  of 2.1 and 8.6 nM, respectively) and a high selectivity over the  $A_1$  and  $A_{2A}$  ARs, but they still do not possess the same outstanding affinity/selectivity profile of their homologue, **5m**.

Compounds **5m**, **5o**, **5p**, and **5r** were also tested at the  $A_{2B}$  AR by evaluating their inhibitory effects on NECA-mediated cAMP accumulation in CHO cells stably expressing this receptor subtype (Table 3). These derivatives were inactive in this assay, thus indicating a complete lack of affinity for  $A_{2B}$  AR.

Given the recent discovery of non-nucleoside AR agonists,<sup>38,39</sup> the antagonistic activities of compounds **5m**, **5o**, **5p**, and **5r** were evaluated in cAMP functional assays at the  $A_3$  AR (Table 3). As expected, all of these compounds displayed full antagonism with potencies comparable to their binding affinities. Furthermore, when tested in the absence of the receptor agonist NECA, they did not show any significant effect on cAMP levels, even following stimulation by forskolin, indicating neutral antagonism (Figure 3).

**Table 2.** Affinities at Human A<sub>1</sub>, A<sub>2A</sub>, and A<sub>3</sub> ARs of Derivatives of 4-Amino-6-hydroxy-2-mercaptopyrimidines **5a–s**

compd	R	R'	R''	K <sub>i</sub> (nM) or % inhibition <sup>a</sup>		
				hA <sub>1</sub> <sup>b</sup>	hA <sub>2A</sub> <sup>c</sup>	hA <sub>3</sub> <sup>d</sup>
<b>5a</b>	CH <sub>3</sub>	CH <sub>3</sub>	CH <sub>3</sub>	30%	29%	49%
<b>5b</b>	CH <sub>3</sub>	CH <sub>3</sub>	CH <sub>3</sub> CH <sub>2</sub>	2%	21%	51%
<b>5c</b>	CH <sub>3</sub>	CH <sub>3</sub> CH <sub>2</sub> CH <sub>2</sub>	CH <sub>3</sub>	7%	1121 ± 88	31 ± 2.4
<b>5d</b>	CH <sub>3</sub>	CH <sub>3</sub> CH <sub>2</sub> CH <sub>2</sub>	CH <sub>3</sub> CH <sub>2</sub>	19%	398 ± 20	45 ± 0.9
<b>5e</b>	CH <sub>3</sub> CH <sub>2</sub> CH <sub>2</sub>	CH <sub>3</sub>	CH <sub>3</sub>	43%	10%	166 ± 10
<b>5f</b>	CH <sub>3</sub> CH <sub>2</sub> CH <sub>2</sub>	CH <sub>3</sub>	CH <sub>3</sub> CH <sub>2</sub>	486 ± 34	4%	276 ± 24
<b>5g</b>	CH <sub>3</sub> CH <sub>2</sub> CH <sub>2</sub>	CH <sub>3</sub> CH <sub>2</sub> CH <sub>2</sub>	CH <sub>3</sub>	5474 ± 275	30%	26 ± 0.8
<b>5h</b>	CH <sub>3</sub> CH <sub>2</sub> CH <sub>2</sub>	CH <sub>3</sub> CH <sub>2</sub> CH <sub>2</sub>	CH <sub>3</sub> CH <sub>2</sub>	1462 ± 111	71 ± 3.4	38 ± 0.7
<b>5i</b>	C <sub>6</sub> H <sub>5</sub> CH <sub>2</sub>	CH <sub>3</sub> CH <sub>2</sub> CH <sub>2</sub>	CH <sub>3</sub>	34%	23%	525 ± 21
<b>5j</b>	CH <sub>3</sub> CH <sub>2</sub> CH <sub>2</sub>	C <sub>6</sub> H <sub>5</sub> CH <sub>2</sub>	CH <sub>3</sub>	2445 ± 110	36%	7.5 ± 0.22
<b>5k</b>	CH <sub>3</sub> CH <sub>2</sub> CH <sub>2</sub>	2-ClC <sub>6</sub> H <sub>4</sub> CH <sub>2</sub>	CH <sub>3</sub>	1840 ± 18	4149 ± 400	6.3 ± 0.07
<b>5l</b>	CH <sub>3</sub> CH <sub>2</sub> CH <sub>2</sub>	3-ClC <sub>6</sub> H <sub>4</sub> CH <sub>2</sub>	CH <sub>3</sub>	582 ± 36.3	41%	7.1 ± 0.48
<b>5m</b>	CH <sub>3</sub> CH <sub>2</sub> CH <sub>2</sub>	4-ClC <sub>6</sub> H <sub>4</sub> CH <sub>2</sub>	CH <sub>3</sub>	17%	43%	3.5 ± 0.05
<b>5n</b>	CH <sub>3</sub> CH <sub>2</sub> CH <sub>2</sub>	2,4-Cl <sub>2</sub> -C <sub>6</sub> H <sub>3</sub> CH <sub>2</sub>	CH <sub>3</sub>	46%	29%	30 ± 2.7
<b>5o</b>	CH <sub>3</sub> CH <sub>2</sub> CH <sub>2</sub>	4-MeOC <sub>6</sub> H <sub>4</sub> CH <sub>2</sub>	CH <sub>3</sub>	2443 ± 240	47%	1.8 ± 0.15
<b>5p</b>	CH <sub>3</sub> CH <sub>2</sub> CH <sub>2</sub>	C <sub>6</sub> H <sub>5</sub> CH <sub>2</sub> CH <sub>2</sub>	CH <sub>3</sub>	2080 ± 205	27%	1.4 ± 0.14
<b>5q</b>	CH <sub>3</sub> CH <sub>2</sub> CH <sub>2</sub>	c-Hex-CH <sub>2</sub>	CH <sub>3</sub>	43%	33%	22 ± 0.4
<b>5r</b>	CH <sub>3</sub> CH <sub>2</sub>	4-ClC <sub>6</sub> H <sub>4</sub> CH <sub>2</sub>	CH <sub>3</sub>	4480 ± 440	56%	2.0 ± 0.2
<b>5s</b>	CH <sub>3</sub> (CH <sub>2</sub> ) <sub>3</sub>	4-ClC <sub>6</sub> H <sub>4</sub> CH <sub>2</sub>	CH <sub>3</sub>	0%	26%	8.6 ± 0.81

<sup>a</sup> The K<sub>i</sub> values are the mean ± SEM of at least three determinations derived from an iterative curve-fitting procedure (Prism program, GraphPad, San Diego, CA). The % inhibition of specific radioligand binding is determined at 10 μM (A<sub>1</sub> and A<sub>2A</sub> ARs), and 1 μM (A<sub>3</sub> ARs) ligand concentration. <sup>b</sup> Displacement of specific [<sup>3</sup>H]DPCPX binding in membranes obtained from CHO cells stably expressing hA<sub>1</sub> AR. See K<sub>i</sub> values of reference ligands in Table 1. <sup>c</sup> Displacement of specific [<sup>3</sup>H]NECA binding in membranes obtained from CHO cells stably expressing hA<sub>2A</sub> AR. See K<sub>i</sub> values of reference ligands in Table 1. <sup>d</sup> Displacement of specific [<sup>125</sup>I]AB-MECA binding in membranes obtained from CHO cells stably expressing hA<sub>3</sub> AR. See K<sub>i</sub> values of reference ligands in Table 1.

**Table 3.** Potency of Compounds **5o**, **5m**, **5p**, and **5r** versus hA<sub>2B</sub> and hA<sub>3</sub> ARs

compd	R	R'	R''	IC <sub>50</sub> <sup>a</sup> (nM) of cAMP assays	
				for hA <sub>2B</sub> CHO cells	for hA <sub>3</sub> CHO cells
<b>5m</b>	CH <sub>3</sub> CH <sub>2</sub> CH <sub>2</sub>	4-ClC <sub>6</sub> H <sub>4</sub> CH <sub>2</sub>	CH <sub>3</sub>	> 10000 (0%)	9.2 ± 0.7
<b>5o</b>	CH <sub>3</sub> CH <sub>2</sub> CH <sub>2</sub>	4-MeOC <sub>6</sub> H <sub>4</sub> CH <sub>2</sub>	CH <sub>3</sub>	> 10000 (0%)	2.7 ± 0.2
<b>5p</b>	CH <sub>3</sub> CH <sub>2</sub> CH <sub>2</sub>	C <sub>6</sub> H <sub>5</sub> CH <sub>2</sub> CH <sub>2</sub>	CH <sub>3</sub>	> 10000 (13%)	1.25 ± 0.09
<b>5r</b>	CH <sub>3</sub> CH <sub>2</sub>	4-ClC <sub>6</sub> H <sub>4</sub> CH <sub>2</sub>	CH <sub>3</sub>	> 10000 (10%)	1.84 ± 0.1

<sup>a</sup> The data are expressed as the mean ± SEM of four independent experiments performed in triplicate. In parentheses are indicated the percentages of inhibition, at 10 μM compound, of the cAMP levels, stimulated by 100 nM NECA for A<sub>2B</sub> adenosine receptors.

The most potent compound at the A<sub>3</sub> AR, **5p**, was docked into our recently published model of this receptor<sup>40</sup> according to a procedure described in the Experimental Section. As shown in Figure 4, **5p** is engaged in several attractive interactions: the ether oxygen receives an H-bond from the N250 (6.55) side chain; the pyrimidine moiety π-stacks with the aromatic rings of H95 (3.37) and W243 (6.48); the phenethyl and the propylthio substituents fill two adjacent hydrophobic pockets delimited by the side chains of F182 (5.43) and W185 (5.46) and of M99 (3.41), L102 (3.44), W185 (5.46), P189 (5.50), and F239 (6.44), respectively. The putative binding mode of **5p** is consistent with the mutagenesis data supporting a key role of H95 (3.37), F182 (5.43), W243 (6.48), and N250 (6.55) in the recognition of several A<sub>3</sub> AR antagonists.<sup>41</sup> This model will probably be

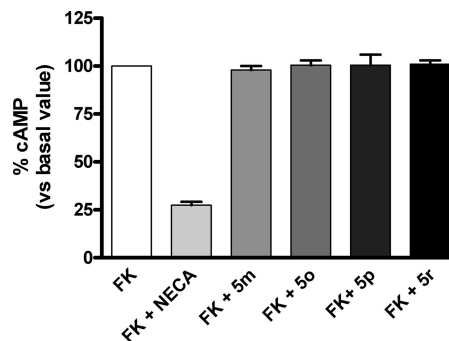


**Figure 3.** Effect of selected compounds (**5m**, **5o**, **5p**, and **5r**) on forskolin (FK) stimulated cAMP production in A<sub>3</sub> CHO cells. Cells were treated with 1 μM forskolin in the absence or in the presence of 100 nM NECA or 10 μM of each compound. Data are expressed as percentage of cAMP production with respect to FK-stimulated cAMP levels, set to 100%. Each data point represents the mean ± SEM of three different experiments.

exploited to design new A<sub>3</sub> AR antagonists similar to our pyrimidine derivatives. A glance at the Y-like disposition of the three substituents of **5p** within the A<sub>3</sub> AR binding cavity may suggest why compounds of series **6** are devoid of any affinity toward this receptor: their R' and R substituents are too close, with the result that the former is forced to clash with the binding cleft boundaries.

In summary, we prepared derivatives of 4-amino-6-hydroxy-2-mercaptopyrimidine (**5**) as open chain analogues of the weakly potent A<sub>3</sub> AR antagonist triazolopyrimidinone derivative (**E**). The optimum size/lipophilicity of the R, R', and R'' substituents born by the new scaffold were sought by a preliminary factorial design followed by a stepwise lead optimization. As a result, we identified **5m** as the ligand displaying the best combination



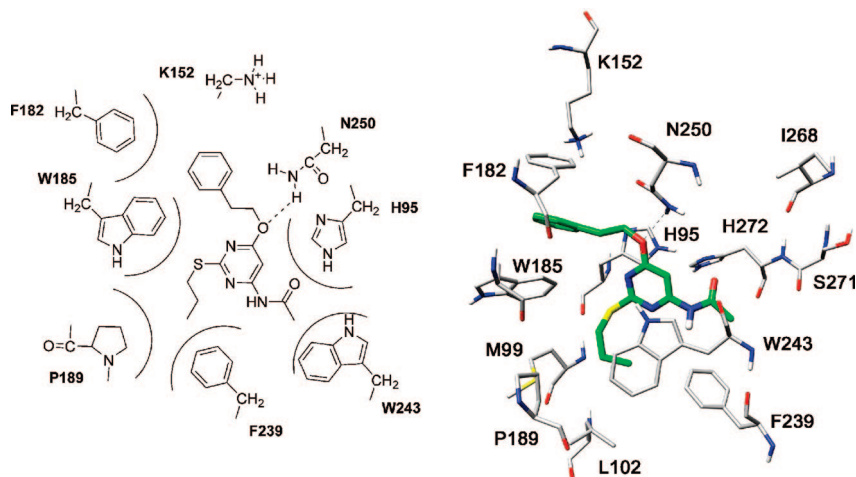


**Figure 4.** Compound **5p** docked into the  $A_3$  AR model.<sup>40</sup>

of potency at the  $A_3$  AR ( $K_i = 3.5$  nM) and selectivity ( $K_i > 10$   $\mu$ M at the  $A_1$  and  $A_{2A}$  ARs).

### Experimental Section

**Chemistry.** Evaporation was performed in vacuo (rotary evaporator). Analytical TLC was carried out on Merck 0.2 mm precoated silica gel aluminum sheets (60 F-254). Silica gel 60 (230–400 mesh) was used for column flash chromatography. Melting points were determined using a Büchi apparatus B 540 and are uncorrected. Routine nuclear magnetic resonance spectra were recorded on a Varian Mercury 400 spectrometer operating at 400 MHz for the proton and 100 MHz for the carbon in DMSO- $d_6$  solution. Elemental analyses were performed by our Analytical Laboratory in Pisa, and the results agreed with theoretical values to within  $\pm 0.4\%$ .

**General Procedure for the Synthesis of 4-Amino-6-hydroxy-2-(phenyl)alkylthiopyrimidines 2a–e.** Haloalkane (12.4 mmol) was added dropwise into a solution of 4-amino-6-hydroxy-2-mercaptopyrimidine monohydrate (1g, 6.2 mmol) in 1 M NaOH (12.4 mL). The reaction mixture was kept, under stirring, at 50–55 °C for 4 h and then was left overnight at room temperature. Next, the mixture was neutralized with acetic acid, obtaining a solid that was collected by filtration, washed with petroleum ether, and dried. The solid, identified by  $^1\text{H}$  and  $^{13}\text{C}$  NMR spectra or by comparison with published melting points<sup>42,43</sup> (see Table 1 of Supporting Information for details), was sufficiently pure to be used in the next reaction without further purification.

**General Procedure for the Synthesis of 6-Amino-3-(phenyl)alkyl-2-(phenyl)alkylthiopyrimidin-4-ones 3a–p and 4-Amino-6-(phenyl)alkoxy-2-(phenyl)-alkylthiopyrimidines 4a–p.** Haloalkane (10.0 mmol) was added dropwise into a suspension of the opportune compound **2a–e** (10.0 mmol) in anhydrous DMF (30 mL) and  $\text{K}_2\text{CO}_3$  (30 mmol). The reaction mixture was kept, under stirring, at 80–85 °C for 4 h. After the mixture was cooled, the inorganic material was taken off by filtration and the solvent was removed in vacuo. The solid residue, consisting of a mixture of **3** and **4** isomers, was resolved by flash chromatography. Purification conditions, yields, and physicochemical and spectral data are reported in Tables 2 and 3 of the Supporting Information.

**General Procedure for the Synthesis of Compounds 5a–s.** A mixture of amine **4a–p** (1.2 mmol), acetic or propionic anhydride (72 mmol), and a catalytic amount of concentrated  $\text{H}_2\text{SO}_4$  was warmed to 50 °C until disappearance of the substrate (40–120 min), while the progress of the reaction was monitored by TLC. After cooling at room temperature, the mixture was poured into ice/water and extracted with chloroform. The organic phase was washed with a saturated solution of  $\text{NaHCO}_3$ , then with water, and dried on  $\text{Na}_2\text{SO}_4$ . Removal of the solvent under reduced pressure gave the crude products **5a–s**, which were purified by recrystallization from *n*-hexane (Table 4 of Supporting Information).

**Biological Methods. Materials.** [ $^3\text{H}$ ]DPCPX, [ $^3\text{H}$ ]NECA, and [ $^{125}\text{I}$ ]AB-MECA were obtained from DuPont-NEN (Boston, MA). Adenosine deaminase (ADA) was from Sigma Chemical Co. (St. Louis, MO). All other reagents were from standard commercial sources and of the highest commercially available grade. CHO cells stably expressing human  $A_1$ ,  $A_{2A}$ ,  $A_{2B}$ , and  $A_3$  receptors were kindly supplied by Prof. K. N. Klotz, Würzburg University, Germany.<sup>44</sup>

**Adenosine Receptor Binding Assay. Human  $A_1$  Adenosine Receptors.** Aliquots of membranes (50  $\mu$ g proteins) obtained from  $A_1$  CHO cells were incubated at 25 °C for 180 min in 500  $\mu$ L of  $T_1$  buffer (50 mM Tris-HCl, 2 mM  $\text{MgCl}_2$ , 2 units/mL ADA, pH 7.4) containing [ $^3\text{H}$ ]DPCPX (3 nM) and six different concentrations of the newly synthesized compounds. Nonspecific binding was determined in the presence of 50  $\mu$ M RPIA.<sup>36</sup> The dissociation constant ( $K_d$ ) of [ $^3\text{H}$ ]DPCPX  $A_1$  CHO cell membranes was 3 nM.

**Human  $A_{2A}$  Adenosine Receptors.** Aliquots of cell membranes (80  $\mu$ g) were incubated at 25 °C for 90 min in 500  $\mu$ L of  $T_2$  buffer (50 mM Tris-HCl, 2 mM  $\text{MgCl}_2$ , 2 units/mL ADA, pH 7.4) in the presence of 30 nM of [ $^3\text{H}$ ]NECA and six different concentrations of the newly synthesized compounds. Nonspecific binding was determined in the presence of 100  $\mu$ M NECA.<sup>36</sup> The dissociation constant ( $K_d$ ) of [ $^3\text{H}$ ]NECA in  $A_{2A}$  CHO cell membranes was 30 nM.

**Human  $A_3$  Adenosine Receptors.** Aliquots of cell membranes (40  $\mu$ g) were incubated at 25 °C for 90 min in 100  $\mu$ L of  $T_3$  buffer (50 mM Tris-HCl, 10 mM  $\text{MgCl}_2$ , 1 mM EDTA, 2 units/mL ADA, pH 7.4) in the presence of 1.4 nM [ $^{125}\text{I}$ ]ABMECA and six different concentrations of the newly synthesized compounds. Nonspecific binding was determined in the presence of 50  $\mu$ M R-PIA.<sup>36</sup> The dissociation constant ( $K_d$ ) of [ $^{125}\text{I}$ ]AB-MECA in  $A_3$  CHO cell membranes was 1.4 nM.

**Measurement of Cyclic AMP Levels on  $hA_{2B}$  and  $hA_3$  CHO Cells.** Intracellular cAMP levels were measured using a competitive protein binding method.<sup>37</sup> (Nordstedt) CHO cells expressing recombinant  $hA_{2B}$  or  $hA_3$  ARs were harvested by trypsinization. After centrifugation and resuspension in medium, cells (~60 000) were plated in 24-well plates in 0.5 mL of medium. After 48 h, the medium was removed, and the cells were incubated at 37 °C for 15 min with 0.5 mL of DMEM in the presence of Ro20-1724 (20  $\mu$ M), as phosphodiesterase inhibitor, and ADA (1U/mL). The antagonistic profile of the new compounds toward  $A_{2B}$  AR was evaluated assessing their ability to inhibit 100 nM NECA-mediated accumulation of cAMP. The antagonistic profile of the new compounds toward  $A_3$  AR was evaluated by assessing their ability to counteract 100 nM NECA-mediated inhibition of cAMP accumulation stimulated by 1  $\mu$ M forskolin. Cells were incubated in the reaction medium (15 min at 37 °C) with different compound concentrations (1 nM to 10  $\mu$ M) and then treated with NECA. In parallel, aliquots of cells were treated with the compound alone (10  $\mu$ M) in the absence or in the presence of forskolin. The reaction

was terminated by removal of the medium and addition of 0.4 N HCl. After 30 min, lysates were neutralized with 4 N KOH, and the suspension was centrifuged at 800g for 5 min. For determination of cAMP production, cAMP binding protein isolated from bovine adrenal glands was incubated with [<sup>3</sup>H]cAMP (2 nM), 50 μL of cell lysate, or cAMP standard (0–16 pmol) at 4 °C for 150 min in a total volume of 300 μL. Bound radioactivity was separated by rapid filtration through GF/C glass fiber filters and washed twice with 4 mL of 50 mM Tris-HCl, pH 7.4. The radioactivity was measured by liquid scintillation spectrometry.

All compounds were routinely dissolved in DMSO and diluted with assay buffer to the final concentration, where the amount of DMSO never exceeded 2%. Percentage inhibition values of specific radiolabeled ligand binding at 1–10 μM concentration are the mean ± SEM of at least three determinations. For compound IC<sub>50</sub> determination, at least six different ligand concentrations were used. IC<sub>50</sub> values, computer-generated using a nonlinear regression formula on a computer program (Graph-Pad, San Diego, CA), were converted to K<sub>i</sub> values, based on the K<sub>d</sub> values of radioligands in the different tissues and using the Cheng and Prusoff equation.<sup>45</sup> K<sub>i</sub> values are the mean ± SEM of at least three determinations.

**Computational Methods.** The ligands were submitted to 1000 steps of Monte Carlo based conformational search employing the MMFFs force field with a distance-dependent dielectric constant of 1.0.<sup>46</sup> The resulting molecules were then energy-minimized using the conjugated gradient method until a convergence value of 0.05 kcal/(mol·Å) was reached. The obtained structures were docked into a recently published<sup>40</sup> model of the A<sub>3</sub> receptor using the AUTODOCK 3.0 program.<sup>47</sup> The regions of interest used by AUTODOCK were defined by considering N250 as the central residue of a grid of 44, 54, and 50 points in the x, y, and z directions. A grid spacing of 0.375 Å and a distance-dependent function of the dielectric constant were used for the energetic map calculations.

By use of a Lamarckian genetic algorithm, the compounds were subjected to 100 runs of the AUTODOCK search with 500 000 steps of energy evaluation; the other parameters were set to default values. Cluster analysis was performed on the docked results, applying an rms tolerance of 1.0 Å.

The best docking complexes were energy-minimized by applying a constraint of 30 kcal/(mol·Å) on the α carbons of the TMs. Each minimization consisted of 5000 steps with a combined algorithm, namely, the sequential steepest descent and conjugate gradient methods for the first 1000 and the last 4000 steps, respectively.

The resulting geometry-optimized complexes were then subjected to 1.2 ns of molecular dynamics (MD) simulation using AMBER 9.0.<sup>48</sup> MD simulations were carried out at 300 K using the parm94 force field. Chlorine ions were added as counterions to neutralize the system. The time step of the simulations was 2.0 fs, with a cutoff of 12 Å for the nonbonded interaction, and the SHAKE option was employed to keep all bonds involving hydrogen atoms rigid. The MD simulation was carried out by gradually decreasing the constraint on the α carbons of the TMs from 30 to 5 kcal/(mol·Å).

The final structure of each complex was obtained by minimizing the average structure of the last 400 ps of MD using the conjugate gradient method until a convergence of 0.05 kcal/(Å·mol) was reached. During the whole computational simulation, with the exception of the α carbons of the TMs, all the atoms were allowed to move. The root-mean-square deviation of all the heavy atoms between the initial complexes and the final structures was about 2.5 Å.

For specific amino acids, both the sequence number and the numbering system proposed by Ballesteros and Weinstein<sup>49</sup> (in parentheses) were employed. For the latter, the most highly conserved residue in each TM helix (TMH) was assigned a value of 0.50, and this number was preceded by the TMH number. The other residues in the helix were given a locant value relative to this.

**Acknowledgment.** This work was financially supported by MIUR (Cofin 2005, ex 40%). We thank Prof. Dr. Karl-Norbert

Klotz for his generous gift of transfected CHO cells expressing human A<sub>1</sub>, A<sub>2A</sub>, A<sub>2B</sub>, and A<sub>3</sub> receptors.

**Supporting Information Available:** Tables listing yields, chemical–physical properties, and spectral data of compounds **2a–e**, **3a–o**, **4a–o**, and **5a–s**, as well as analytical data of **5a–s**. This material is available free of charge via the Internet at <http://pubs.acs.org>.

## References

- Poulsen, S.-A.; Quinn, R. J. Adenosine Receptors: New Opportunities for Future Drugs. *Bioorg. Med. Chem.* **1998**, *6*, 619–641.
- Fredholm, B. B.; Arslan, G.; Halldner, L.; Kull, B.; Schulte, G.; Wasserman, W. Structure and Function of Adenosine Receptors and Their Genes. *Naunyn-Schmiedeberg's Arch. Pharmacol.* **2000**, *362*, 364–374.
- Fredholm, B. B.; IJzerman, A. P.; Jacobson, K. A.; Klotz, K.-N.; Linden, J. International Union of Pharmacology. XXV. Nomenclature and Classification of Adenosine Receptors. *Pharmacol. Rev.* **2001**, *53*, 527–552.
- Salvatore, C. A.; Jacobson, M. A.; Taylor, H. E.; Linden, J.; Johnson, R. G. Molecular Cloning and Characterization of the Human A<sub>3</sub> Adenosine Receptor. *Proc. Natl. Acad. Sci. U.S.A.* **1993**, *90*, 10365–10369.
- Linden, J.; Taylor, H. E.; Robeva, A. S.; Tucker, A. L.; Stehle, J. H.; Rivkees, S. A.; Fink, J. S.; Reppert, S. M. Molecular Cloning and Functional Expression of a Sheep A<sub>3</sub> Adenosine Receptor with Widespread Tissue Distribution. *Mol. Pharmacol.* **1993**, *44*, 524–532.
- Ji, X.-D.; Von Lubitz, D.; Olah, M. E.; Stiles, G. L.; Jacobson, K. A. Species Differences in Ligand Affinity at Central A<sub>3</sub>-Adenosine Receptors. *Drug Dev. Res.* **1994**, *33*, 51–59.
- Schulte, G.; Fredholm, B. B. Signalling from Adenosine Receptors to Mitogen-Activated Protein Kinases. *Cell. Signalling* **2003**, *15*, 813–827.
- Jacobson, K. A.; Gao, Z.-G. Adenosine Receptors As Therapeutic Targets. *Nat. Rev. Drug Discovery* **2006**, *5*, 247–264.
- Moro, S.; Gao, Z.-G.; Jacobson, K. A.; Spalluto, G. Progress in the Pursuit of Therapeutic Adenosine Receptor Antagonists. *Med. Chem. Res.* **2006**, *26*, 131–159.
- Brambilla, R.; Cattabeni, F.; Ceruti, S.; Barbieri, D.; Franceschi, C.; Kim, Y.-C.; Jacobson, K. A.; Klotz, K.-N.; Lohse, M. J.; Abbracchio, M. P. Activation of the A<sub>3</sub> Adenosine Receptor Affects Cell Cycle Progression and Cell Growth. *Naunyn-Schmiedeberg's Arch. Pharmacol.* **2000**, *361*, 225–234.
- Linden, J. Cloned Adenosine A<sub>3</sub> Receptors: Pharmacological Properties, Species Differences and Receptor Functions. *Trends Pharmacol. Sci.* **1994**, *15*, 298–306.
- Liang, B. T.; Jacobson, K. A. A Physiological Role of the Adenosine A<sub>3</sub> Receptor: Sustained Cardioprotection. *Proc. Natl. Acad. Sci. U.S.A.* **1998**, *95*, 6995–6999.
- Akkari, R.; Burbiel, J. C.; Hockemeyer, J.; Müller, C. E. Recent Progress in the Development of Adenosine Receptor Ligands as Antiinflammatory Drugs. *Curr. Top. Med. Chem.* **2006**, *6*, 1375–1399.
- Mitchell, C. H.; Peterson-Yantorno, K.; Carré, D. A.; McGlinn, A. M.; Coca-Prados, M.; Stone, R. A.; Civan, M. M. A<sub>3</sub> Adenosine Receptors Regulate Cl<sup>-</sup> Channels of Nonpigmented Ciliary Epithelial Cells. *Am. J. Physiol.* **1999**, *276*, 659–666.
- Baraldi, P. G.; Tabrizi, M. A.; Romagnoli, R.; Fruttarolo, F.; Merighi, S.; Varani, K.; Gessi, S.; Borea, P. A. Pyrazolo[4,3-*e*]1,2,4-Triazolo[1,5-*c*]Pyrimidine Ligands, New Tools to Characterize A<sub>3</sub> Adenosine Receptors in Human Tumor Cell Lines. *Curr. Med. Chem.* **2005**, *12*, 1319–1329.
- Gessi, S.; Cattabriga, E.; Avitabile, A.; Gafà, R.; Lanza, G.; Cavazzini, L.; Bianchi, N.; Gambari, R.; Feo, C.; Liboni, A.; Gullini, S.; Leung, E.; Mac-Lennan, S.; Borea, P. A. Elevated Expression of A<sub>3</sub> Adenosine Receptors in Human Colorectal Cancer Is Reflected in Peripheral Blood Cells. *Clin. Cancer Res.* **2004**, *10*, 5895–5901.
- Fishman, P.; Bar-Yehuda, S. Pharmacology and Therapeutic Applications of A<sub>3</sub> Receptor Subtype. *Curr. Top. Med. Chem.* **2003**, *3*, 463–469.
- Merighi, S.; Mirandola, P.; Varani, K.; Gessi, G.; Capitani, S.; Leung, E.; Baraldi, P. G.; Tabrizi, M. A.; Borea, P. A. Pyrazolotriazolopyrimidine Derivatives Sensitive Melanoma Cells to the Chemotherapeutic Drugs: Taxol and Vindesine. *Biochem. Pharmacol.* **2003**, *66*, 739–748.
- Müller, C. E.; Thorand, M.; Qurishi, R.; Diekmann, M.; Jacobson, K. A.; Padgett, W. L.; Daly, J. W. Imidazo[2,1-*i*]purin-5-ones and Related Tricyclic Water-Soluble Purine Derivatives: Potent A<sub>2A</sub>- and A<sub>3</sub>-Adenosine Receptor Antagonists. *J. Med. Chem.* **2002**, *45*, 3440–3450.

- (20) Müller, C. E. *Medicinal Chemistry of Adenosine A<sub>3</sub> Receptor Ligands. Curr. Top. Med. Chem.* **2003**, *3*, 445–462.
- (21) Francis, J. E.; Cash, W. D.; Psychoyos, S.; Ghai, G.; Wenk, P.; Friedmann, R. C.; Atkins, C.; Warren, V.; Furness, P.; Hyun, J. L.; Stone, G. A.; Desai, M.; Williams, M. Structure–Activity Profile of a Series of Novel Triazoloquinazoline Adenosine Antagonists. *J. Med. Chem.* **1988**, *31*, 1014–1020.
- (22) Kim, Y.-C.; Ji, X.-D.; Jacobson, K. A. Derivatives of the Triazoloquinazoline Adenosine Antagonist (CGS 15943) Are Selective for the Human A<sub>3</sub> Receptor Subtypes. *J. Med. Chem.* **1996**, *39*, 4142–4148.
- (23) Baraldi, P. G.; Cacciari, B.; Romagnoli, R.; Merighi, S.; Varani, K.; Borea, P. A.; Spalluto, G. A<sub>3</sub> Adenosine Receptor Ligands: History and Perspectives. *Med. Res. Rev.* **2000**, *20*, 103–128.
- (24) Baraldi, P. G.; Cacciari, B.; Borea, P. A.; Varani, K.; Pastorin, G.; Da Ros, T.; Tabrizi, M. A.; Fruttarolo, F.; Spalluto, G. Pyrazolo-Triazolo-Pyrimidine Derivatives as Adenosine Receptor Antagonists: A Possible Template for Adenosine Receptor Subtypes. *Curr. Pharm. Des.* **2002**, *8*, 2299–2332.
- (25) Colotta, V.; Catarzi, D.; Varano, F.; Cecchi, L.; Filacchioni, G.; Martini, C.; Trincavelli, L.; Lucacchini, A. 1,2,4-Triazolo[4,3-*a*]quinoxalin-1-one: A Versatile Tool for the Synthesis of Potent and Selective Adenosine Receptor Antagonists. *J. Med. Chem.* **2000**, *43*, 1158–1164.
- (26) Colotta, V.; Catarzi, D.; Varano, F.; Calabri, F. R.; Lenzi, O.; Filacchioni, G.; Martini, C.; Trincavelli, L.; Deflorian, F.; Moro, S. 1,2,4-Triazolo[4,3-*a*]quinoxalin-1-one Moiety as an Attractive Scaffold to Develop New Potent and Selective Human A<sub>3</sub> Adenosine Receptor Antagonists: Synthesis, Pharmacological, and Ligand–Receptor Modeling Studies. *J. Med. Chem.* **2004**, *47*, 3580–3590.
- (27) Catarzi, D.; Colotta, V.; Varano, F.; Calabri, F. R.; Lenzi, O.; Filacchioni, G.; Trincavelli, L.; Martini, C.; Tralli, A.; Monopoli, C.; Moro, S. 2-Aryl-8-chloro-1,2,4-triazolo[1,5-*a*]quinoxalin-4-amines as Highly Potent A<sub>1</sub> and A<sub>3</sub> Adenosine Receptor Antagonists. *Bioorg. Med. Chem.* **2005**, *13*, 705–715.
- (28) Van Muijlwijk-Koezen, J. E.; Timmerman, H.; Link, R.; van der Goot, H.; IJzerman, A. P. A Novel Class of Adenosine A<sub>3</sub> Receptor Ligands. 1. 3-(2-Pyridinyl)isoquinoline Derivatives. *J. Med. Chem.* **1998**, *41*, 3987–3993.
- (29) Van Muijlwijk-Koezen, J. E.; Timmerman, H.; Link, R.; van der Goot, H.; IJzerman, A. P. A Novel Class of Adenosine A<sub>3</sub> Receptor Ligands. 2. Structure Affinity Profile of a Series of Isoquinoline and Quinazoline Compounds. *J. Med. Chem.* **1998**, *41*, 3994–4000.
- (30) Van Muijlwijk-Koezen, J. E.; Timmerman, H.; van der Goot, H.; Menge, W. M. P. B.; von Drabbe Künzel, J. F.; de Groote, M.; IJzerman, A. P. Isoquinoline and Quinazoline Urea Analogues as Antagonists for the Human Adenosine A<sub>3</sub> Receptor. *J. Med. Chem.* **2000**, *43*, 2227–2238.
- (31) Li, A.-H.; Moro, S.; Melman, N.; Ji, X. D.; Jacobson, K. A. Structure–Activity Relationships and Molecular Modeling of 3,5-Diacyl-2,4-dialkylpyridine Derivatives as Selective A<sub>3</sub> Adenosine Receptor Antagonists. *J. Med. Chem.* **1998**, *41*, 3186–3201.
- (32) Li, A.-H.; Moro, S.; Forsyth, N.; Melman, N.; Ji, X. D.; Jacobson, K. A. Synthesis, CoMFA Analysis, and Receptor Docking of 3,5-Diacyl-2,4-dialkylpyridine Derivatives as Selective A<sub>3</sub> Adenosine Receptor Antagonists. *J. Med. Chem.* **1999**, *42*, 706–721.
- (33) Van Rhee, A. M.; Jiang, J. L.; Melman, N.; Olah, M. E.; Stiles, G. L.; Jacobson, K. A. Interaction of 1,4-Dihydropyridine and Pyridine Derivatives with Adenosine Receptors: Selectivity for A<sub>3</sub> Receptors. *J. Med. Chem.* **1996**, *39*, 2980–2989.
- (34) Novellino, E.; Cosimelli, B.; Ehlardo, M.; Greco, G.; Iadanza, M.; Lavecchia, A.; Rimoli, M. G.; Sala, A.; Da Settimo, A.; Primofiore, G.; Da Settimo, F.; Taliani, S.; La Motta, C.; Klotz, K.-N.; Tuscano, D.; Trincavelli, M. L.; Martini, C. 2-(Benzimidazol-2-yl)quinoxalines: A Novel Class of Selective Antagonists at Human A<sub>1</sub> and A<sub>3</sub> Adenosine Receptors Designed by 3D Database Searching. *J. Med. Chem.* **2005**, *48*, 8253–8260.
- (35) Allen, F. H.; Bellard, S.; Brice, M. D.; Cartwright, B. A.; Doubleday, A.; Higgs, H.; Hummelink, T.; Hummelink-Peters, B. G.; Kennard, O.; Motherwell, W. D. S.; Rodgers, J. R.; Watson, D. G. The Cambridge Crystallographic Data Centre: Computer-Based Search, Retrieval, Analysis and Display of Information. *Acta Crystallogr.* **1979**, *B35*, 2231–2239.
- (36) Da Settimo, F.; Primofiore, G.; Taliani, S.; La Motta, C.; Novellino, E.; Greco, G.; Lavecchia, A.; Cosimelli, B.; Iadanza, M.; Klotz, K.-N.; Tuscano, D.; Trincavelli, M. L.; Martini, C. A1 Adenosine Receptor Antagonists, 3-Aryl[1,2,4]triazinobenzimidazol-4-(10*H*)-ones (ATBIs) and *N*-Alkyl and *N*-Acyl-(7-substituted-2-phenylimidaz[1,2-*a*][1,3,5]triazin-4-yl)amines (ITAs): Different Recognition of Bovine and Human Binding Sites. *Drug Dev. Res.* **2004**, *63*, 1–7.
- (37) Nordstedt, C.; Fredholm, B. B. A Modification of a Protein-Binding Method for Rapid Quantification of cAMP in Cell-Culture Supernatants and Body Fluid. *Anal. Biochem.* **1990**, *189*, 231–234.
- (38) Beukers, M. W.; Chang, L. C. W.; von Frijtag Drabbe Künzel, J. D.; Mulder-Krieger, T.; Spanjersberg, R. F.; Brussee, J.; IJzerman, A. P. New, Non-Adenosine, High-Potency Agonists for the Human Adenosine A<sub>2B</sub> Receptor with an Improved Selectivity Profile Compared to the Reference Agonist *N*-Ethylcarboxamidoadenosine. *J. Med. Chem.* **2004**, *47*, 3707–3709.
- (39) Chang, L. C. W.; von Frijtag Drabbe Künzel, J. D.; Mulder-Krieger, T.; Spanjersberg, R. F.; Roerink, S. F.; van den Hout, G.; Beukers, M. W.; Brussee, J.; IJzerman, A. P. A Series of Ligands Displaying a Remarkable Agonistic–Antagonistic Profile at the Adenosine A<sub>1</sub> Receptor. *J. Med. Chem.* **2005**, *48*, 2045–2053.
- (40) Tafi, A.; Bernardini, C.; Botta, M.; Corelli, F.; Andreini, M.; Martinelli, A.; Ortore, G.; Baraldi, P. G.; Fruttarolo, F.; Borea, P. A.; Tuccinardi, T. Pharmacophore Based Receptor Modeling: The Case of Adenosine A<sub>3</sub> Receptor Antagonists. An Approach to the Optimization of Protein Models. *J. Med. Chem.* **2006**, *49*, 4085–4097.
- (41) Martinelli, A.; Tuccinardi, T. Molecular Modeling of Adenosine Receptors: New Results and Trends. *Med. Res. Rev.*, published online 2007, DOI 10.1002/med.20106.
- (42) Tsuji, T.; Watanabe, S.; Nakadai, Y.; Toyoshima, S. Synthesis and Antimicrobial Activity of *N*-(2-Alkylthio-6-alkoxy-4-pyrimidinyl)-sulfanilamide. *Chem. Pharm. Bull.* **1962**, *10*, 9–13.
- (43) Gibson, C. L.; La Rosa, S.; Ohta, K.; Boyle, P. H.; Leurquin, F.; Lemaçon, A.; Suckling, C. J. The Synthesis of 7-Deazaguanines as Potential Inhibitors of Guanosine Triphosphate Cyclohydrolase I. *Tetrahedron* **2004**, *60*, 943–959.
- (44) Klotz, K.-N.; Hessling, J.; Hegler, J.; Owman, C.; Kull, B.; Fredholm, B. B.; Lohse, J. Comparative Pharmacology of Human Adenosine Receptor Subtypes–Characterization of Stably Transfected Receptors in CHO Cells. *Naunyn-Schmiedeberg's Arch. Pharmacol.* **1998**, *357*, 1–9.
- (45) Cheng, Y.-C.; Prusoff, W. H. Relationship between the Inhibition Constant (K<sub>i</sub>) and the concentration of inhibitor which causes 50 per cent inhibition (I<sub>50</sub>) of an enzymatic reaction. *Biochem. Pharmacol.* **1973**, *22*, 3099–3108.
- (46) *Macromodel*, version 8.5; Schrödinger Inc.: New York, 1999.
- (47) Morris, G. M.; Goodsell, D. S.; Halliday, R. S.; Huey, R.; Hart, W. E.; Belew, R. K.; Olson, A. J. Automated docking using a Lamarckian genetic algorithm and empirical binding free energy function. *J. Comput. Chem.* **1998**, *19*, 1639–1662.
- (48) Case, D. A.; Darden, T. A.; Cheatham, T. E., III; Simmerling, C. L.; Wang, J.; Duke, R. E.; Luo, R.; Merz, K. M.; Pearlman, D. A.; Crowley, M.; Walker, R. C.; Zhang, W.; Wang, B.; Hayik, S.; Roitberg, A.; Seabra, G.; Wong, K. F.; Paesani, F.; Wu, X.; Brozell, S.; Tsui, V.; Gohlke, H.; Yang, L.; Tan, C.; Mongan, J.; Hornak, V.; Cui, G.; Beroza, P.; Mathews, D. H.; Schafmeister, C.; Ross, W. S.; Kollman, P. A. *AMBER 9*; University of California: San Francisco, CA, 2006.
- (49) Ballesteros, J. A.; Weinstein, H. W. Integrated Methods for the Construction of Three-Dimensional Models and Computational Probing of Structure–Function Relations in G-Protein Coupled Receptors. *Methods Neurosci.* **1995**, *25*, 366–428.

JM701159T